



Full length article

GPS signal acquisition via compressive multichannel sampling

Xiao Li^{a,*}, Andrea Rueetschi^a, Yonina C. Eldar^b, Anna Scaglione^a^a University of California, Davis, United States^b Technion - Israel Institute of Technology, Haifa, Israel

ARTICLE INFO

Article history:

Received 17 January 2011

Received in revised form 9 July 2011

Accepted 18 July 2011

Available online 16 September 2011

Keywords:

GPS

Compressive sensing

Spread spectrum

Analog compressed sensing

ABSTRACT

In this paper, we propose an efficient acquisition scheme for GPS receivers. It is shown that GPS signals can be effectively sampled and detected using a bank of randomized correlators with much fewer chip-matched filters than those used in existing GPS signal acquisition algorithms. The latter use correlations with all possible shifted replicas of the satellite-specific C/A code and an exhaustive search for peaking signals over the delay-Doppler space. Our scheme is based on the recently proposed analog compressed sensing framework, and consists of a multichannel sampling structure with far fewer correlators.

The compressive multichannel sampler outputs are linear combinations of a vector whose support tends to be sparse; by detecting its support one can identify the strongest satellite signals in the field of view and pinpoint the correct code-phase and Doppler shifts for finer resolution during tracking. The analysis in this paper demonstrates that GPS signals can be detected and acquired via the proposed structure at a lower cost in terms of number of correlations that need to be computed in the coarse acquisition phase, which in current GPS technology scales like the product of the number of all possible delays and Doppler shifts. In contrast, the required number of correlators in our compressive multichannel scheme scales as the number of satellites in the field of view of the device times the logarithm of number of delay-Doppler bins explored, as is typical for compressed sensing methods.

© 2011 Elsevier B.V. All rights reserved.

1. Introduction

Nowadays, Global Positioning System (GPS) chips are ubiquitous, and continue to be embedded in a variety of devices. A GPS device allows to determine its location with about 3 meters accuracy, by measuring the propagation delay of signals transmitted by the set of GPS satellites in the field of view (FOV) of any receiver located on the surface of the earth, which typically requires measurements from at least four satellites [1].

Conventionally, the signal that arrives at the receiver is downconverted, match-filtered and oversampled at a

fast rate. Subsequently, the receiver acquires enough (at least four) strong signals by exploiting the orthogonality of the distinct *coarse/acquisition* (C/A) codes used in GPS signaling at each satellite [2]. However, due to the unknown propagation delays, the samples obtained are misaligned in time and therefore, it is vital to pinpoint the code-phase in order to decode the navigation data correctly [2,3] and use the time-delay information for pseudo-range computation. Furthermore, each of the satellites contributes a component of the received GPS signal that is characterized by a distinct Doppler offset [4], due to the unequal relative velocities of the satellites and the receiver, as well as the offsets of the different local oscillators at the GPS receivers. In general, time-frequency synchronization as well as signal detection is tackled in GPS receivers during the *acquisition/detection* stage via a parallel search over the binned delay-Doppler space across all the satellite C/A codes [5,6].

* Corresponding author.

E-mail addresses: eceli@ucdavis.edu (X. Li), arueetschi@ucdavis.edu (A. Rueetschi), yonina@ee.technion.ac.il (Y.C. Eldar), ascaglione@ucdavis.edu (A. Scaglione).

In many practical scenarios, signals might arrive at the receiver with multipath components instead of the line of sight (LOS) component [3,6,7]. Constructive and destructive superpositions of randomly delayed and faded replicas, leads to distorted correlation peaks. This is usually tackled in the *tracking stage* [2] that follows the *acquisition/detection* stage, by using an *early-late* receiver. Such a receiver compares the energy of a symbol period in the first half from the early gate to the energy in the last half from the late gate so that the receiver can synchronize the signals accordingly. Furthermore, many approaches, in addition to the early-late structure, have been proposed to better mitigate the effects brought by multipath, including (but not limited to) the Narrow Correlator [8], Multipath Eliminating Technique (MET) [9], and Multipath Estimating Delay Lock Loop (MEDLL) [10]. These methods differ in their capabilities to remove multipath errors, specifically at low signal-to-noise ratio (SNR) and/or in the presence of interference. In this work, we start from the general signal model that considers multipath effects and propose an acquisition scheme that coarsely captures significant paths for each active satellite, with its corresponding code-phase and Doppler. The tracking stage that further resolves the estimates of delay-Doppler pairs as well as the multipath components is beyond the scope of this paper.

As described above, the acquisition and detection of GPS signals is usually performed sequentially. First, the strongest signals coming from the satellites are detected by searching a binned delay-Doppler space via exhaustive correlations that pinpoint the correct coarse timing delays and frequency offsets. After acquisition and detection, the signal is locked and the device enters the tracking stage that tackles fine synchronization and multipath error mitigation in order to despread, demodulate and decode the navigation data correctly in real-time. However, this acquisition/detection scheme can be computationally intensive due to the large number of correlations, and especially the exhaustive search for peaks over the binned delay-Doppler space across all the satellite signals with distinct C/A codes. For example, the maximum Doppler shift in a GPS signal is typically within $[-10 \text{ kHz}, 10 \text{ kHz}]$ and the search step size is usually 500 Hz while the maximum delay can run up to a C/A code length 1023. In this case, the 2D delay-Doppler peak is found by comparing the outputs of $1023 \times 41 \approx 4 \times 10^4$ correlators for each satellite, which is a heavy computation burden.

Paper contributions: In order to scale down the operations and hardware requirements, we propose a simple and efficient acquisition scheme based on the recently developed compressed sensing (CS) framework [11] and its extension to analog signals [12]. The multichannel samplers in [12] are constructed as a linear combination of the duals of all the generators, where the generators in this case correspond to the satellite-specific C/A code waveforms. In our context, we show that the duals of the generators are well approximated by the generators themselves. This alleviates one of the most difficult aspects in the practical application of [12], namely, the physical implementation of the dual filters, by exploiting properties of the spread spectrum sequences that are used in GPS systems. Thanks to

this interpretation, the proposed multichannel samplers can be viewed as performing independent random projections of all correlators outputs. The resulting set of compressive measurements are then used together to recover the peaks located sparsely over the delay-Doppler space, which is a jointly sparse recovery problem with infinite input vectors and infinite measurement vectors (IMVs). The continuous-to-finite (CTF) method introduced in [13] effectively reduces the IMV problem to a finite multiple measurement vector (MMV) system with jointly sparse inputs, which can be solved efficiently using the Reduce MMV and Boost (ReMBo) technique proposed in [13], or other MMV approaches [14,15].

The paper is organized as follows. Section 2 describes the general model for GPS signals. Section 3 re-interprets existing GPS acquisition schemes from a sampling point of view. In order to scale down the computations and hardware requirements, Section 4 introduces the analog CS framework. In Section 5 we further reduce the general solution to a set of simple compressive samplers by utilizing the structure of GPS signals. Numerical results are shown in Section 6 to demonstrate the effectiveness of our proposed acquisition scheme, followed by a complexity analysis given in Section 7. Finally the paper is concluded in Section 8.

2. GPS signal model

The signal transmitted by the satellites is a direct sequence spread spectrum (DS-SS) signal modulated onto L_1 and L_2 frequencies at 1575.42 MHz and 1227.60 MHz respectively. In commercial GPS systems publicly available to civilian users, the DS-SS signal received at the user end is carried on L_1 frequency from all the available launched satellites. Equivalently, the baseband signal from the i th satellite is transmitted as

$$s_i(t) = \sum_{n \in \mathbb{Z}} d_i[n] \phi_i(t - nT), \quad i = 1, \dots, I \quad (1)$$

where $\phi_i(t)$ is a spreading waveform determined by a satellite-specific spreading code and $\{d_i[n]\}_{n \in \mathbb{Z}}$ is the navigation data sent by the i th satellite with a symbol period of T , containing its time stamp, orbit location and relevant information entailed for positioning the receiver.

More specifically, the waveform $\phi_i(t)$ is determined by the i th satellite's C/A code $\{s_i[m]\}$ as

$$\phi_i(t) = \sum_{m=0}^{M-1} s_i[m] g(t - mT_c), \quad i = 1, \dots, I \quad (2)$$

where $g(t)$ is a wideband short pulse. For simplicity, we assume that $g(t)$ has a flat spectrum of bandwidth $\Omega_g = 2\pi L/T_c$ (typically $L = 1$) approximated with error $\epsilon_g(\omega)$

$$G(\omega) = [1 + \epsilon_g(\omega)] \text{rect}_{2\pi L/T_c}(\omega), \quad (3)$$

where $\epsilon_g(\omega)$ specifies the deviation from the flat spectrum with $\|\epsilon_g(\omega)\| \ll 1$. Due to the periodicity of the C/A

¹ The notation $\|\cdot\|$ refers to the L_2 norm of a function $\|\epsilon_g(\omega)\| \triangleq \sqrt{\int_{-\infty}^{\infty} |\epsilon_g(\omega)|^2 d\omega}$.

code, $T = MT_c$. The C/A code $\{s_i[m]\}$ is a pseudo-random binary sequence of length M that contains N maximum length sequences (MLSs) or Gold sequences of length $M_0 = 1023$ transmitted with a chip period $T_c = 977.5$ ns, which implies $M = NM_0$. In fact, by the GPS transmission standards we have $N = 20$ for the GPS L1-C/A signal, i.e. $T = 20$ ms.

The correlation properties of the spreading code are vital in the recovery of spread spectrum signals. Denote the cross-correlation between different C/A codes as

$$R_{i'i}[u] \triangleq \frac{1}{M} \sum_{m=0}^{M-1} s_{i'}[m-u] s_i^*[m]. \quad (4)$$

When M is large, the Gold sequences or MLS sequences are orthogonal between different satellites and approximately orthogonal between different shifts [7,16] such that $R_{i'i}[u] = 1$ when $u = 0, i = i'$ while $\mathcal{O}(1/M)$ otherwise. This is indicated by the flat $2\pi/T_c$ -periodic cross spectral density

$$S_{i'i}(e^{i\omega T_c}) \triangleq \sum_{u=-M+1}^{M-1} R_{i'i}[u] e^{-i\omega u T_c} = \delta[i' - i] + \epsilon_{i'}(\omega), \quad (5)$$

where the error function $\epsilon_{i'}(\omega)$ is also $2\pi/T_c$ -periodic with $\|\epsilon_{i'}(\omega)\| \ll 1$. This flat property plays an essential role in simplifying the design presented later in this paper.

After downconversion, the signal at the receiver can be modeled as

$$x(t) = \sum_{i=1}^I \sum_{r=1}^R h_{i,r} s_i(t - \tau_{i,r}) e^{i\omega_{i,r} t} + v(t), \quad (6)$$

where $\{h_{i,r}\}_{r=1,\dots,R}$ are the multipath channel taps with delays $\{\tau_{i,r}\}_{r=1,\dots,R}$ and Doppler shifts $\{\omega_{i,r}\}_{r=1,\dots,R}$ from the i th satellite to the receiver, and $v(t)$ is Additive White Gaussian Noise (AWGN) with variance σ^2 . Combined with the signal model (1), the signal $x(t)$ is represented as

$$x(t) = \sum_{n \in \mathbb{Z}} \sum_{i=1}^I \sum_{r=1}^R a_{i,r}[n] \phi_i(t - nT - \tau_{i,r}) e^{i\omega_{i,r} t} + v(t),$$

where $a_{i,r}[n] \triangleq h_{i,r} d_i[n]$. In the coarse acquisition phase, it is typically assumed that the delays are integer multiples of the chip duration $\tau_{i,r} = q_{i,r} T_c$ with $q_{i,r} \in \mathcal{Q}$ and the Doppler shifts are integer multiples of the frequency search step $\omega_{i,r} = k_{i,r} \Delta\omega$ with $k_{i,r} \in \mathcal{K}$, where the sets \mathcal{Q} and \mathcal{K} define the delay-Doppler space. This leads to the following discretized signal model

$$x(t) = \sum_{n \in \mathbb{Z}} \sum_{i=1}^I \sum_{r=1}^R a_{i,r}[n] \phi_i(t - nT - q_{i,r} T_c) \times e^{i k_{i,r} \Delta\omega t} + v(t). \quad (7)$$

3. Standard GPS acquisition scheme

The main task of the acquisition stage is to detect the correct code-phase $\mathbf{q} \triangleq \{q_{i,r}\}_{i=1,\dots,I}^{r=1,\dots,R}$ and Doppler shift

$\mathbf{k} \triangleq \{k_{i,r}\}_{i=1,\dots,I}^{r=1,\dots,R}$ across the delay-Doppler space and recover the sequence $\{a_{i,r}[n]\}_{i=1,\dots,I}$, among which the strongest set \mathcal{I} of satellites ($|\mathcal{I}| \geq 4$) are picked for the purpose of triangulation [1–4]. Note that the sequence $\{a_{i,r}[n]\}_{n \in \mathbb{Z}}$ includes the attenuation of the channels between the satellites and the receiver. Therefore, its magnitude indicates the strength of the signal received and only the strong ones are acquired by the receiver. In general, the magnitudes of those acquired $i \in \mathcal{I}$ are significantly greater than those $i \notin \mathcal{I}$, making the coefficients $a_{i,r}[n]$ sparse over i due to the wide difference in signal strength.

3.1. Exhaustive search via matched filtering (MF)

Conventionally, the acquisition and detection of strong satellite signals is achieved by correlating the incoming signal $x(t)$ with a bank of match-filters $\phi_i(t)$'s that are separately modulated by carriers $\{e^{i k \Delta\omega t}\}_{k \in \mathcal{K}}$ and shifted in time $\{\phi_i(t - q T_c)\}_{q \in \mathcal{Q}}$. In this way, the paths corresponding to peaks in the magnitude of $a_{i,r}[n]$ can be found in the delay-Doppler binned-space $\mathcal{Q} \times \mathcal{K}$ for each satellite corresponding to its C/A code.

This approach can be viewed as sampling with a set of filters, followed by uniform sampling at times $t = nT$, as depicted in Fig. 1. The sampling kernels of this equivalent structure are given by $\phi_{i,k,q}(t) = \phi_i(t - q T_c) e^{i k \Delta\omega t}$, for all $i = 1, \dots, I, k \in \mathcal{K}$ and $q \in \mathcal{Q}$. The sampled output in each channel is equal to

$$z_{i,k,q}[n] \triangleq \langle x(t), \phi_{i,k,q}(t - nT) \rangle. \quad (8)$$

In the Fourier domain, we have

$$Z_{i,k,q}(e^{i\omega T}) = \frac{1}{T} \sum_{\ell \in \mathbb{Z}} \Phi_{i,k,q}^* \left(\omega - \frac{2\pi \ell}{T} \right) X \left(\omega - \frac{2\pi \ell}{T} \right), \quad (9)$$

where $\Phi_{i,k,q}^*(\omega)$ and $X(\omega)$ are the Fourier transforms of $\phi_{i,k,q}(-t)$ and $x(t)$ respectively. Note that the summation over $\ell \in \mathbb{Z}$ in (9) depends on the bandwidth of the filter $\phi_{i,k,q}(-t)$, where as mentioned in Section 2 the bandwidth of $g(t)$ is $\Omega_g = 2\pi LM/T$. Therefore, the summation becomes finite from $\ell = 0$ to $\ell = LM - 1$ over $\omega \in [-\pi/T, \pi/T]$. From (7), we can express $X(\omega)$ as

$$X(\omega) = \sum_{i=1}^I \sum_{r=1}^R A_{i,r}(e^{i\omega T}) \Phi_i(\omega - k_{i,r} \Delta\omega) \times e^{-i(\omega - k_{i,r} \Delta\omega) q_{i,r} T_c} + V(e^{i\omega T}), \quad (10)$$

where we defined $A_{i,r}(e^{i\omega T}) \triangleq \sum_{n \in \mathbb{Z}} a_{i,r}[n] e^{-in(\omega - k_{i,r} \Delta\omega) T}$. Substituting (10) into (9), and denoting by $\mathbf{z}(e^{i\omega T})$ the length- $I|\mathcal{K}||\mathcal{Q}|$ column vector whose (i, k, q) th element is $Z_{i,k,q}(e^{i\omega T})$, and by $\mathbf{a}_i(e^{i\omega T})$ the length- R column vector of $\{A_{i,r}(e^{i\omega T})\}_{r=1,\dots,R}$ for the i th data stream, we can write

$$\mathbf{z}(e^{i\omega T}) = \mathbf{M}_{\phi\phi}(\omega, \mathbf{k}, \mathbf{q}) \mathbf{a}(e^{i\omega T}) + \mathbf{v}(e^{i\omega T}) \quad (11)$$

over the domain $\omega \in [-\pi/T, \pi/T]$. The derivation is identical to the development in [17] and is therefore omitted. Here $\mathbf{a}(e^{i\omega T}) \triangleq [\mathbf{a}_1^H(e^{i\omega T}), \dots, \mathbf{a}_I^H(e^{i\omega T})]^H$ is a length- IR vector containing the DFT of all the data sequences

² The norm here is defined as $\|\epsilon_{i'}(\omega)\| \triangleq \int_{-\pi/T_c}^{\pi/T_c} |\epsilon_{i'}(\omega)|^2 d\omega$ due to the periodicity.

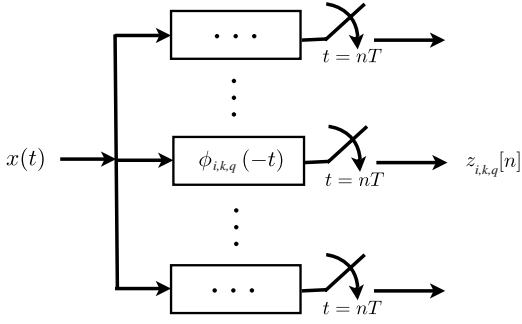


Fig. 1. Exhaustive matched filtering (MF) approach.

$\{a_{i,r}[n]\}_{n \in \mathbb{Z}}$, and $\mathbf{M}_{\phi\phi}(\omega, \mathbf{k}, \mathbf{q})$ is an $I|\mathcal{K}||\mathcal{Q}| \times IR$ sub-matrix with the (i, r) th column being the $(i, k_{i,r}, q_{i,r})$ th column from the $I|\mathcal{K}||\mathcal{Q}| \times I|\mathcal{K}||\mathcal{Q}|$ full Gram matrix $\mathbf{M}_{\phi\phi}(\omega, \mathcal{K}, \mathcal{Q})$ of all the generators

$$\begin{aligned} & [\mathbf{M}_{\phi\phi}(\omega, \mathcal{K}, \mathcal{Q})]_{(i',k',q'),(i,k,q)} \\ &= \frac{1}{T} \sum_{\ell=0}^{LM-1} \Phi_{i',k',q'}^* \left(\omega - \frac{2\pi\ell}{T} \right) \Phi_{i,k,q} \left(\omega - \frac{2\pi\ell}{T} \right). \quad (12) \end{aligned}$$

The component $\mathbf{v}(e^{i\omega T}) = [\dots, v_{i,k,q}(e^{i\omega T}), \dots]^T$ is the filtered noise by MFs (generators) $\{\phi_{i,k,q}(t)\}_{i=1,\dots,I}^{k \in \mathcal{K}, q \in \mathcal{Q}}$ and therefore has a cross-spectral density matrix $\mathbf{R}_{vv}(e^{i\omega T}) = \sigma^2 \mathbf{M}_{\phi\phi}(\omega, \mathcal{K}, \mathcal{Q})$.

Exploiting the specific choice of sampling kernels and the structure of $\mathbf{M}_{\phi\phi}(\omega, \mathbf{k}, \mathbf{q})$ and $\mathbf{M}_{\phi\phi}(\omega, \mathcal{K}, \mathcal{Q})$, we can further analyze the output samples $\mathbf{z}(e^{i\omega T})$ as stated below.

Theorem 1. Suppose that the following conditions hold:

- (C1) the pulse shaping filter has a spectrum $G(\omega) = [1 + \epsilon_g(\omega)] \text{rect}_{2\pi L/T_c}(\omega)$ with error $\epsilon_g(\omega)$;
- (C2) the C/A code cross spectral density is $S_{i'i}(e^{i\omega T_c}) = \delta[i' - i] + \epsilon_{i'i}(\omega)$ with error $\epsilon_{i'i}(\omega)$;
- (C3) the frequency search step size is chosen as $\Delta\omega = 2\pi j/T$ and $j \in \mathbb{Z}^+$.

If the error functions satisfy $\|\epsilon_g(\omega)\| \ll 1$ and $\|\epsilon_{i'i}(\omega)\| \ll 1$ for any $i', i = 1, \dots, I$, then the Gram matrix of all the generators $\{\phi_i(t - qT_c)e^{ik\Delta\omega t}\}_{i=1,\dots,I}^{k \in \mathcal{K}, q \in \mathcal{Q}}$ satisfies

$$\mathbf{M}_{\phi\phi}(\omega, \mathcal{K}, \mathcal{Q}) = LM\mathbf{I} + \mathbf{E}(\omega), \quad (13)$$

where $\mathbf{E}(\omega)$ is a bounded perturbation matrix satisfying $\|\mathbf{E}(\omega)\|_{(i',k',q'),(i,k,q)} = \mathcal{O}(1) \ll LM$. The output samples $\mathbf{z}[n] = [\dots, z_{i,k,q}[n], \dots]^T$ at each of the kernels $\phi_{i,k,q}(t)$ can be written as

$$z_{i,k,q}[n] = \begin{cases} LMa_{i,r}[n] + \mathcal{O}(1) + v_{i,k,q}[n], & q = q_{i,r} \text{ and } k = k_{i,r} \\ \mathcal{O}(1) + v_{i,k,q}[n], & \text{otherwise,} \end{cases}$$

where $v_{i,k,q}[n]$ is the filtered noise sample with covariance $\mathbb{E}\{v_{i,k,q}^*[n]v_{i',k',q'}[n]\} = LM\sigma^2\delta[i - i']\delta[k - k']\delta[q - q'] + \mathcal{O}(1)$ and $\mathcal{O}(1) \ll LM$ is some bounded perturbation error with LM being the processing gain on the signal-to-noise ratio.

Proof. See the Appendix. \square

Note that the frequency step size $\Delta\omega = 2\pi j/T$ corroborates the fact that for standard commercial GPS systems, the step size is usually $2\pi \times 500$ rads/s which fits the analysis here by choosing $j = 10$. Also, we can see that the output $z_{i,k,q}[n]$ at each sampler represents the correlation between the MFs and the incoming signal, which is proportional to the magnitude of $a_{i,r}[n]$ and corrupted by noise. Assuming large enough processing gain LM and small enough noise, the delay-Doppler pairs $\{\tau_{i,r} = q_{i,r}T_c\}_{i=1,\dots,I}^{r=1,\dots,R}$ and $\{\omega_{i,r} = k_{i,r}\Delta\omega\}_{i=1,\dots,I}^{r=1,\dots,R}$ can be found by the locations of the peak/dominant entries in $z_{i,k,q}[n]$. The strongest set of satellite signals can then be detected by comparing the values in $z_{i,k,q}[n]$ so that a subset \mathcal{L} of the satellite signals are locked and passed onto the tracking stage for finer extraction. If we ignore the noise for a moment, then $z_{i,k,q}[n]$ is sparse in the sense that for each value n it contains only a small number of non-zero entries.

3.2. Compressive multichannel acquisition

Although effective, this conventional approach taken by standard GPS receivers performs exhaustive correlations (MF approach) that requires abundant samples from a large number of correlators $I|\mathcal{Q}||\mathcal{K}|$. This task can be computationally expensive and demanding on the hardware and memory resources. Assuming a maximum channel delay spread of $\tau_{\max} = QT_c$ and Doppler shift of $|\omega_{\max}| = K\Delta\omega$, the total number of correlators is $2IQK$. For example, the maximum Doppler shift is typically ± 10 kHz. Assuming a delay spread up to code length $\tau_{\max} = MT_c$, then with a frequency grid of 500 Hz, the total number of correlators needed becomes $24 \times 1023 \times 41 \approx 10^6$.

Therefore, it is highly desirable to scale down the computational complexity and power consumption of a user GPS device by performing less correlations while sustaining its capability to pinpoint the signal timing and Doppler information during acquisition. By observing the correlation outputs in the vector $\mathbf{z}[n] = [\dots, z_{i,k,q}[n], \dots]^T$, it can be seen that only few of the dominant entries are useful. Our goal is to exploit the underlying sparsity in the signal model to design an acquisition scheme that requires far fewer correlators. Instead of tackling the problem from a MF viewpoint as in standard GPS, we look at the problem from an analog CS perspective [12], which is one of the main contributions of this paper.

The analog CS design outlined in [12] requires a small number of samplers (only twice the sparsity $2|J|R$ in a noiseless setting), and hence gives rise to substantial practical savings as analyzed later in Section 7. However, the solution [12] is given in the frequency domain and in general does not admit a tractable form in time domain, which makes it hard to implement in practice. Another contribution of this work lies in further exploiting the structure of GPS signals so that the sampling kernels are easy to implement. The outputs from the compressive samplers can then be used to solve the sparse recovery problem of locating the dominant/peak values reflected in the vector $\mathbf{z}[n]$, for example, using the method in [13].

Before we go into the details of our design, we start by describing the analog CS framework [12]. In Section 5 we further develop and simplify the general solution to fit our problem.

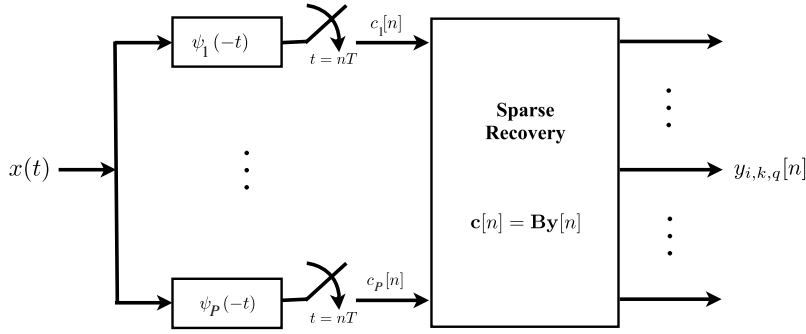


Fig. 2. Compressive multichannel sampling (CS) approach.

4. Compressed sensing of analog signals

The exhaustive MF approach in standard GPS receivers acquires delays and Dopplers by directly exposing the sparse structure in the output samples $\mathbf{z}[n]$ obtained from a large number of correlators. In order to reduce the number of correlators while retaining the ability to correctly identify the peaks of $\mathbf{z}[n]$, it is possible to directly measure a compressed version of $\mathbf{z}[n]$ at the sampler outputs and recover that sparse structure instead, by employing analog CS techniques.

4.1. General model for analog compressed sensing (CS)

The signal model in (7) does not reflect any sparse structure, since it is expressed by a set of deterministic generators $\phi_i(t)$'s defined by unknown parameters $q_{i,r}$ and $k_{i,r}$. The sparsity we exploit is the sparsity of delay-Doppler pairs pinpointed by the peak/dominant entries in $\mathbf{z}[n]$ over the entire delay-Doppler space $\mathcal{Q} \times \mathcal{K}$ for each user $i = 1, \dots, I$ that is informative in acquiring the signal. Using a dictionary $\{\phi_i(t - qT_c)e^{ik\Delta\omega t}\}_{k \in \mathcal{K}, q \in \mathcal{Q}}$, the signal can be equivalently expressed by

$$x(t) = \sum_{n \in \mathbb{Z}} \sum_{i=1}^I \sum_{k \in \mathcal{K}} \sum_{q \in \mathcal{Q}} y_{i,k,q}[n] \phi_i(t - nT - qT_c) \times e^{ik\Delta\omega t} + v(t),$$

where

$$y_{i,k,q}[n] = \begin{cases} a_{i,r}[n], & q = q_{i,r} \text{ and } k = k_{i,r} \\ 0, & \text{otherwise.} \end{cases} \quad (14)$$

Note that the sparsity of $\mathbf{y}[n] \triangleq [\dots, y_{i,k,q}[n], \dots]^T$ is identical to that of $\mathbf{z}[n]$ in the noiseless setting. Indeed, for each $i = 1, \dots, I$ there are altogether R dominant coefficients $\{y_{i,k,q}[n]\}_{k \in \mathcal{K}, q \in \mathcal{Q}}$ that correspond to the original coefficients $\{a_{i,r}[n]\}_{r=1, \dots, R}$ and select the correct code-phase $q_{i,r}$ and Doppler shifts $k_{i,r}$. Let the support of $\mathbf{y}[n]$ be \mathcal{S} , so that the support \mathcal{S} contains the code-phase and Doppler information for acquisition, with a sparsity of $|\mathcal{S}| = |\mathcal{K}||\mathcal{Q}|$. The aim of analog CS is to exploit this sparsity in acquiring $x(t)$ using fewer correlators.

4.2. General solution of compressive samplers

The scheme of [12] uses a set of compressive samplers $\psi_p(-t)$, $p = 1, \dots, P \ll |\mathcal{K}||\mathcal{Q}|$ to obtain minimal

measurements, from which the sparse vector $\mathbf{y}[n]$ can be recovered. As depicted in Fig. 2, the samples at the output of $\psi_p(-t)$ at $t = nT$ are given by

$$c_p[n] \triangleq \langle x(t), \psi_p(t - nT) \rangle. \quad (15)$$

Similar to the mathematical manipulations in Section 3, the system equation can be re-written as

$$\mathbf{c}(e^{i\omega T}) = \mathbf{M}_{\psi\phi}(\omega, \mathcal{K}, \mathcal{Q})\mathbf{y}(e^{i\omega T}) + \mathbf{w}(e^{i\omega T}), \quad (16)$$

where $\mathbf{M}_{\psi\phi}(\omega, \mathcal{K}, \mathcal{Q})$ is a $P \times I|\mathcal{K}||\mathcal{Q}|$ matrix with similar structure to (12) and the notation $\mathbf{w}(e^{i\omega T})$ is used to distinguish the noise component from the previous method in standard GPS. It has been proven in [12] that in a noiseless setting, simply twice the sparsity $P = 2|\mathcal{K}||\mathcal{Q}|$ is needed for successful recovery of the sparse vector $\mathbf{y}[n]$, if $\psi_p(-t)$'s are chosen properly. For noisy scenarios, the necessary number of channels P is larger than the minimum, and evaluated numerically; in any case, it is much smaller than that required by the MF scheme, as we will demonstrate in Section 6.

This reduction is obtained by appropriately choosing a set of randomized correlators $\Psi(\omega) \triangleq [\Psi_1(\omega), \dots, \Psi_P(\omega)]^T$. A general expression of the compressive samplers is given in [12] as

$$\Psi(\omega) = \mathbf{B}\mathbf{M}_{\phi\phi}^{-1}(\omega, \mathcal{K}, \mathcal{Q})\Phi(\omega, \mathcal{K}, \mathcal{Q}), \quad (17)$$

where \mathbf{B} is a sensing matrix satisfying certain coherence properties [11] (e.g., Gaussian random matrix or partial DFT matrix [11], or an appropriate deterministic binary matrix [18]), and $\Phi(\omega, \mathcal{K}, \mathcal{Q}) \triangleq [\dots, \Phi_i(\omega - k\Delta\omega)e^{-i(\omega - k\Delta\omega)qT_c}, \dots]^T$ is a length- $I|\mathcal{K}||\mathcal{Q}|$ vector containing the Fourier transforms of the generators $\{\phi_i(t - qT_c)e^{ik\Delta\omega t}\}_{i=1, \dots, I, k \in \mathcal{K}, q \in \mathcal{Q}}$. With this choice of $\Psi(\omega)$, it can be shown that $\mathbf{M}_{\psi\phi}(\omega, \mathcal{K}, \mathcal{Q}) = \mathbf{B}$. Since \mathbf{B} is independent of frequency ω , transforming (16) into the time domain, the samples can be written as

$$\mathbf{c}[n] = \mathbf{B}\mathbf{y}[n] + \mathbf{w}[n], \quad n \in \mathbb{Z}. \quad (18)$$

The vectors $\{\mathbf{y}[n]\}$ are jointly sparse since they all share the same sparsity pattern. To find $\mathbf{y}[n]$, we can convert (18) to a finite MMV problem using the continuous-to-finite (CTF) technique developed in [13]. Specifically, we first find a basis for the range space of $\{\mathbf{c}[n]\}$ by computing the covariance matrix \mathbf{R}_{cc} and decomposing it as $\mathbf{R}_{cc} = \mathbf{C}\mathbf{C}^H$. Here \mathbf{C} can be chosen as the eigenvectors of \mathbf{R}_{cc} multiplied

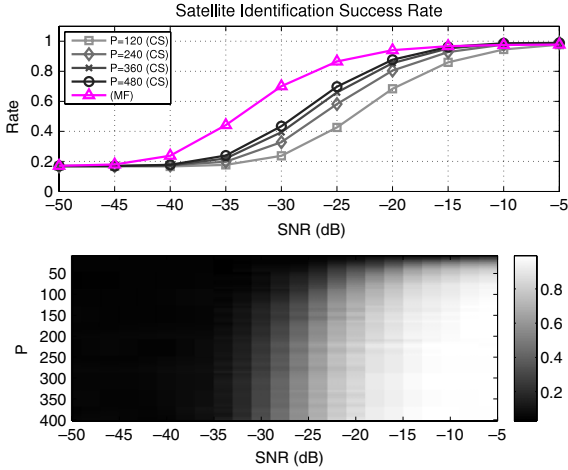


Fig. 3. Satellite identification rate $\mathbb{P}(\hat{\mathcal{I}} = \mathcal{I})$ using a single measurement $\mathbf{c}[1]$ for a CS receiver vs. the MF receiver for $P = \{120, 240, 360, 480\}$ (above), and for $P = \{10, 20, \dots, 400\}$ (below).

by the square-root of the corresponding eigenvalues. Then, the support of $\mathbf{y}[n]$, $n \in \mathbb{Z}$ can be obtained by solving $\mathbf{C} = \mathbf{B}\mathbf{Y}$, where \mathbf{Y} is the sparsest matrix satisfying the measurement equation. This problem can be treated using various MMV sparse recovery techniques [14,15]. In our simulations, we use the ReMBo algorithm developed in [13]. Finally the support of $\mathbf{y}[n]$ is obtained by taking the union of the supports of the columns in the matrix \mathbf{Y} . Once the support of $\mathbf{y}[n]$ is recovered, the acquisition of correct delay-Doppler pair is automatically achieved by locating the dominants/peaks in the vector $\mathbf{y}[n]$ of (14).

Remark. As verified in Section 6, as the number of correlators P increases, the acquisition performance improves significantly. Solving the MMV problem requires collecting multiple measurement vectors $\{\mathbf{c}[n]\}$, while the standard GPS scheme can either employ information for a single measurement $\mathbf{z}[n]$ in (8) or further leverage the processing gain over multiple measurements $\{\mathbf{z}[n]\}$. For the proposed compressive acquisition scheme, if a single vector measurement is used to recover the sparse vector $\mathbf{y}[n]$ using greedy methods or ℓ_1 -norm based methods, the performance will degrade as shown in Fig. 3 but not significantly. Therefore, there is a trade-off between the number of observations $\mathbf{c}[n]$, the number of acquisition channels P as well as the accuracy of the acquisition in comparison with the standard GPS scheme.

5. Simplified compressive samplers

The method proposed in [12] depends on the ability of physically implementing the sampling kernels in (17). Therefore, we explore the structure of the matrix $\mathbf{M}_{\phi\phi}(\omega, \mathcal{K}, \mathcal{Q})$ to provide practical insights on the design of such filters.

Corollary 1. Suppose that (C1)–(C3) and the requirement on the error functions in Theorem 1 hold. Then the sampling

kernels can then be chosen as a linear combination of $\{\phi_i(t - qT_c)e^{ik\Delta\omega t}\}_{i=1,\dots,I}^{k \in \mathcal{K}, q \in \mathcal{Q}}$

$$\psi_p(t) = \sum_{i=1}^I \sum_{k \in \mathcal{K}} \sum_{q \in \mathcal{Q}} b_{p,(i,k,q)} \phi_i(t - qT_c) e^{ik\Delta\omega t},$$

$$p = 1, \dots, P. \quad (19)$$

Proof. From (17) we have the general solution of the compressive samplers

$$\Psi(\omega) = \mathbf{B}\mathbf{M}_{\phi\phi}^{-1}(\omega, \mathcal{K}, \mathcal{Q})\Phi(\omega, \mathcal{K}, \mathcal{Q}). \quad (20)$$

According to the result in Theorem 1, using Taylor expansion on the matrix inverse $\mathbf{M}_{\phi\phi}^{-1}(\omega, \mathcal{K}, \mathcal{Q})$ and ignoring high order terms scaled by $1/LM \ll 1$, we can approximate the inverse by

$$\left(\mathbf{I} + \frac{1}{LM}\mathbf{E}(\omega)\right)^{-1} = \mathbf{I} - \frac{1}{LM}\mathbf{E}(\omega) + \frac{1}{(LM)^2}\mathbf{E}^2(\omega) - \frac{1}{(LM)^3}\mathbf{E}^3(\omega) \cdots \approx \mathbf{I}, \quad (21)$$

where the last approximation comes from the fact that $\mathbf{E}(\omega)$ contains negligible elements. Therefore, the compressive samplers can be chosen directly as $\Psi(\omega) = \mathbf{B}\Phi(\omega, \mathcal{K}, \mathcal{Q})$, which leads to the time-domain expression in the corollary. \square

The filter responses of (19) can be pre-computed, and these P channel outputs are sampled every $T = MT_c$ to produce the test statistics that are going to be used in lieu of the coefficients $\mathbf{z}[n]$ in Theorem 1.

Remark. Note that although the samples are taken at $1/T$, the physical implementation of the compressive multichannel filtering operation is likely to require digital processing at the chip rate $1/T_c$. Nevertheless, it is possible that a wise choice of the coefficients of the matrix \mathbf{B} can further help reduce computations while maintaining the identifiability of the parameters. Analysis of this approach goes beyond our current scope. What we can certainly claim is that the number of computations is now controlled by the parameter P , rather than by the number of possible generators that span all possible delays \mathcal{Q} and Dopplers \mathcal{K} . In fact, the sampling kernels are pre-computed and used online. This is likely to reduce cost of computation, access to memory and storage. The performance of the compressive multichannel sensing structure degrades gracefully as P decreases, giving designers degrees of freedom to choose a desirable operating point.

6. Numerical results

In this section, we run numerical simulations to demonstrate the proposed CS acquisition scheme in GPS receivers. In the simulation, $|\mathcal{I}| = 4$ out of $I = 24$ satellites asynchronously transmit C/A signals that are received by the GPS devices, where length- M Gold sequences are used with $M = NM_0$, $N = 20$ and $M_0 = 1023$. A total of $n = 50$ navigation data bits are sent at the rate of $1/T = 50$ Hz (i.e., $T = 20$ ms). The transmit filter is modeled by a

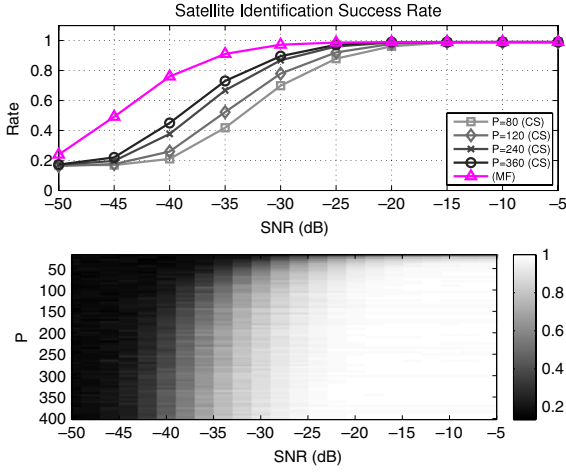


Fig. 4. Satellite identification rate $\mathbb{P}(\hat{\mathcal{I}} = \mathcal{I})$ using a single measurements $\{\mathbf{c}[1], \mathbf{c}[2], \dots, \mathbf{c}[50]\}$ for a CS receiver vs. the MF receiver for $P = \{80, 120, 240, 360\}$ (above), and for $P = \{10, 20, \dots, 400\}$ (below).

finite length pulse shaping filter $g(t) = \sqrt{T_c} \text{sinc}(t/T_c)$ when $|t| \leq T_g$, and $g(t) = 0$ otherwise. The length T_g is sufficiently large so that the response of the pulse in the frequency domain remains approximately flat, i.e. $G(\omega) \approx \text{rect}_{2\pi/T_c}(\omega)$.

To reduce the simulation overhead without incurring a loss of generality, we assume that our statistical model for the channel consists of uniformly distributed delays, $\tau_{i,r} \sim \mathcal{U}(0, \tau_{\max})$ that are bounded by a maximum delay spread of $\tau_{\max} = 20T_c$; and of Doppler shifts, $|\omega_{i,r}| \leq \omega_{\max}$ that are uniformly distributed, $\omega_{i,r} \sim \mathcal{U}(-\omega_{\max}, \omega_{\max})$ over a frequency range delimited by $\omega_{\max}/2\pi = 2.5$ kHz. The channel gains are $h_{i,r} \sim \mathcal{CN}(0, 1)$, with a multi-path propagation having $R = 2$ paths per satellite. In order to identify fractional delays with a half-chip accuracy, the functions $\phi_{i,k,q}(t) = \phi_i(t - qT_c)e^{jk\Delta\omega t}$ are chosen with a half-chip spacing $q = 0, 1/2, 1, \dots$ such that the resolution of $\Delta\tau = T_c/2$ is achieved, and with a frequency resolution of $\Delta\omega = 10 \times 2\pi/T$ that corresponds to steps around 500 Hz when $T = 20$ ms. It follows that $|\mathcal{Q}| = \lceil \tau_{\max}/\Delta\tau \rceil + 1 = 41$ and $|\mathcal{K}| = 2\lceil \omega_{\max}/\Delta\omega \rceil + 1 = 11$. For simulation purpose, the sensing matrix \mathbf{B} is generated as a random binary matrix (while in practice it can be chosen as a deterministic binary matrix to simplify the implementation of correlators [18]).

In all simulations, the attenuated components with distinct delays from each of the satellites are acquired by a number of $P = \{80, 120, 240, 360, 480\}$ channels, in contrast to the traditional $24 \times 41 \times 11 \approx 1 \times 10^4$. The performance is illustrated in terms of success rate and average Root Mean Square Error (RMSE), respectively, in Figs. 3 and 4. The success rate of acquisition is the probability $\mathbb{P}(\hat{\mathcal{I}} = \mathcal{I})$ of the proposed scheme to determine the strongest $|\mathcal{I}| = 4$ signals, which is shown in the figure against the number of channels P and the SNR. The conditional RMSE is an average error between the true delay-frequency parameters and those associated to the strongest paths of the correctly identified satellites

$$\text{RMSE}_{\text{average}}(\mathbf{q}) \triangleq \sqrt{\frac{1}{|\{\hat{\mathcal{I}} \cap \mathcal{I}\}|} \sum_{i \in \{\hat{\mathcal{I}} \cap \mathcal{I}\}} (\hat{q}_i \Delta\tau - \tau_i)^2},$$

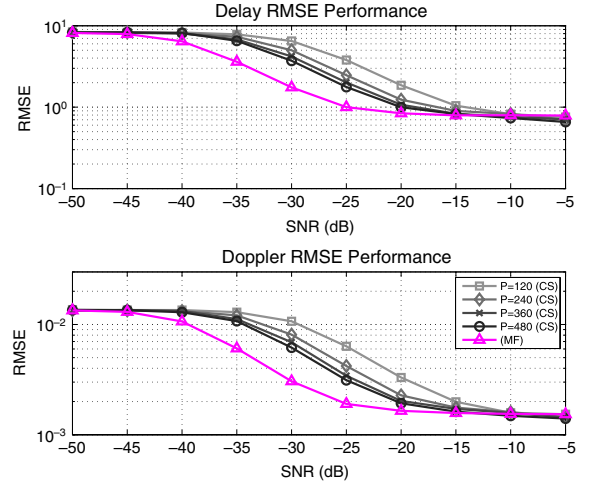


Fig. 5. Delay estimation (above) and Doppler estimation (below) performance of the CS scheme, with $n = 1$ and $P = \{120, 240, 360, 480\}$ compared against the MF receiver.

where $(\tau_i, \omega_i) \triangleq (\tau_{i,r^*}, \omega_{i,r^*})$ with $r^* = \arg \max_{r \in \{1, \dots, R\}} |h_{i,r}|^2$ and

$$(\hat{q}_i, \hat{k}_i) = \arg \max_{q \in \mathcal{Q}, k \in \mathcal{K}} |z_{i,k,q}[n]|^2 = \arg \max_{q \in \mathcal{Q}, k \in \mathcal{K}} |y_{i,k,q}[n]|^2 \quad (22)$$

are the delay-frequency index pairs of strongest path associated to the i th satellite. Similarly, the average RMSE for the Doppler is

$$\text{RMSE}_{\text{average}}(\mathbf{k}) \triangleq \sqrt{\frac{1}{|\{\hat{\mathcal{I}} \cap \mathcal{I}\}|} \sum_{i \in \{\hat{\mathcal{I}} \cap \mathcal{I}\}} (\hat{k}_i \Delta\omega - \omega_i)^2}.$$

Although the compressive acquisition scheme suffers from a compression loss, both Figs. 3 and 4 highlight its ability to perform closely as the traditional MF. When $P \geq 80$ and $\text{SNR} \geq -25$ dB the active satellites \mathcal{I} can be identified satisfactorily which leads to great savings (less than 1% of the original 1×10^4).

The figures above illustrate acquisition performances using a single set of measurements $\mathbf{c}[0]$ against that using multiple sets of measurements $\{\mathbf{c}[n]\}_{n=1}^{50}$. Using a single measurement suffers from a performance loss (-10 dB for $P = 120$ at the rate of approximately 0.8). In fact, by reducing n , the accuracy of $\mathbf{z}[n]$ and consequently the sensitivity, degrade. Furthermore, it can be seen from Fig. 3 that the required number of channels P has to be raised to 480 (less than 5% of the original 1×10^4) to achieve a reliable rate that approaches the MF result.

A similar trend is also visible on the conditional RMSE curves for both single (Fig. 5) and multiple (Fig. 6) modes (-12 dB for $P = 120$ when $\text{RMSE}(\mathbf{q}) \approx 2$ and $\text{RMSE}(\mathbf{k}) \approx 2 \cdot 10^{-3}$). At high SNR the performance is limited by the presence of a systematic error due to the modeling mismatch from the quantized parameters. At low SNR, instead, the error is bounded by the length of the search interval QT_c . Once again the CS method closely approaches the MF performance, especially when $n = 1$.

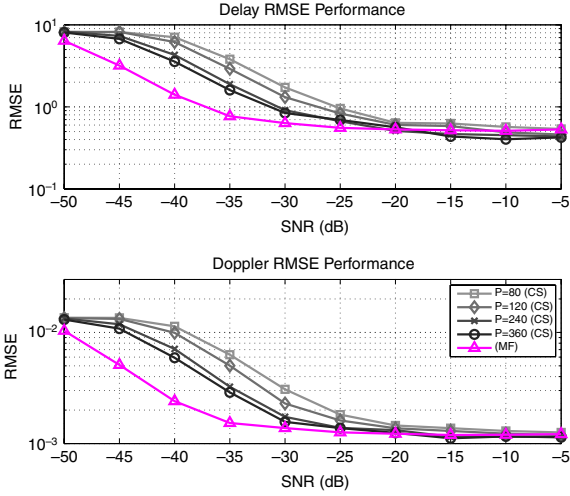


Fig. 6. Delay estimation (above) and Doppler (estimation) performance of the CS scheme, with multiple measures ($n = 50$) and $P = \{80, 120, 240, 360\}$, compared against the MF receiver also processing $n = 50$ measures.

7. Complexity analysis

The complexity of the acquisition algorithm is due to two aspects: (1) *storage requirement* and (2) *computational complexity*. We provide here a brief analysis of the complexity of the proposed CS scheme against the traditional MF scheme. To make a fair and practical comparison, we assume that the implementation is done in the digital domain and we use the L_{kernel} -tap digitized version of the sampling kernels $\{\psi_p(t)\}_{p=1}^P$ (and also $\{\phi_{i,k,q}(t)\}_{i=1,\dots,I}^{k \in \mathcal{K}, q \in \mathcal{Q}}$ for the traditional case).

7.1. Storage and processing requirement

The difference in storage results from two sources, one is the storage for the digital kernel taps and the other is the outputs of the sampling kernels used for peak recovery, both of which are proportional to the number of sampling kernels. Furthermore, the processing overhead per unit of time for these stored values scales proportionally with the storage requirement as well.

	Sampling kernels	Output samples
CS receiver	$P \times L_{\text{kernel}}$	$\mathcal{O}(P)$
MF receiver	$I \mathcal{K} \mathcal{Q} \times L_{\text{kernel}}$	$\mathcal{O}(I \mathcal{K} \mathcal{Q})$

It is clear that the proposed compressive acquisition scheme handles less data, which facilitates the pipelining of the algorithm and also relieves the burden of storage.

7.2. Computational complexity

The difference in computations stems from the correlations and the search for the peak. The number of operations in performing correlations is proportional to the number of sampling kernels, while the peak recovery is different

for the two approaches, depending on how the sparse recovery (proposed CS structure) and the exhaustive search (MF structure) are implemented. Here we further compare the two architectures by their number of operations that are necessary to identify the delay-Doppler pairs (22). In this practical analysis, the compressed samples $\mathbf{c}[n]$ are obtained by post-processing of the digitally sampled versions of $x(t)$ at the chip rate and processed using a greedy algorithm Orthogonal Matching Pursuit (OMP) [19]. Note that using analog implementation in the acquisition can further bring down the complexity in terms of processing.

We introduce a vector $\mathbf{x}[n]$ of M dimensions, whose m th entry is $(\mathbf{x}[n])_m \triangleq x(nT + mT_c)$, to digitally capture and compress one instance of the signal according to

$$c_p[n] \triangleq \langle \mathbf{x}[n], \psi_p[m - nM] \rangle. \quad (23)$$

For the MF receiver, instead, we assume an oversampling ratio of 2 to achieve half chip accuracy, i.e., $\Delta\tau = T_c/2$, and downsize the filterbank array. The sequence $\mathbf{x}[n]$ is partitioned into 2 sub-sequences $\{\mathbf{x}_1[n], \mathbf{x}_2[n]\}$, of M samples each, whose m th element is $\{\mathbf{x}_i[n]\}_m \triangleq x(nT + mT_c + (i-1)T_c/2)$, $i = 1, 2$. A typical filter model would process the stream of $2M$ samples sequentially, however to emulate the block processing nature of the CS receiver and avoid CPU cycles that would further delay the execution of the algorithm, we let the 2 sub-sequences be processed concurrently.

All the arithmetic operations, starting from $\mathbf{x}[n]$, necessary to detect the $|\mathcal{J}|R$ vector elements are recorded and listed in Table 1. The table outlines the computational complexity breakdown for both the MF and the CS schemes using single and multiple measurements (MMV). This popular algorithm seeks the \mathcal{J} (with $|\mathcal{J}| = |\mathcal{J}|R$) non-zero elements of the sparse vector $\mathbf{y}[n]$ by sequentially choosing dictionary elements that better correlate with the observations $\mathbf{c}[n]$. At every iteration the current estimate is subtracted from the observation vector (**OMP.1**) and the residual projected onto the dictionary elements (**OMP.2**). Then, the dictionary element linked to the largest coefficient (**OMP.3**) is retained and removed from the dictionary. The updated set of coefficients is obtained by projecting $\mathbf{c}[n]$ onto the subspace formed by the set of atoms that were removed from the dictionary (**OMP.4**). The algorithm stops when either a maximum number of iterations is reached or when the norm of the residual falls below a predefined threshold (**OMP.5**).

Path selection refers to identifying the support of a certain vector for pinpointing the active components (delay-Doppler pairs). For both CS and MF, it is tightly coupled to the sorting algorithm being implemented and therefore, we only list its average computational complexity rather than the number of comparators.

When the representation of $\mathbf{y}[n]$ is sufficiently sparse, i.e. for GPS applications $|\mathcal{J}| \ll I|\mathcal{K}||\mathcal{Q}|$, the number of operations needed to digitally compress $\mathbf{x}[n]$ into $\mathbf{c}[n]$ and to project the residual of each OMP iteration onto the dictionary (**OMP.2**) dominate the overall complexity of the CS receiver, leading to an order of $\mathcal{O}(nP(M + I|\mathcal{K}||\mathcal{Q}||\mathcal{J}|))$. On the other hand, the number of operations for the MF are

Table 1
Complexity breakdown for the proposed CS and traditional MF acquisition using n sets of measurements.

CS receiver	Complexity	Remarks
Digital compression $c_p[n]$	$\mathcal{O}(nMP)$	Eq. (23)
Covariance \mathbf{R}_{cc} (optional ³)	$\mathcal{O}(nP^2)$	MMV mode
SVD of \mathbf{R}_{cc} (optional ³)	$\mathcal{O}(n^2P)$	$n \leq P$ [20], MMV mode
Residual update	$\mathcal{O}(n \mathcal{J} ^2)$	(OMP.1)
Inner products	$\mathcal{O}(nP \mathcal{K} \mathcal{Q} \mathcal{J})$	(OMP.2)
Maximum projection	$\mathcal{O}(\mathcal{J} \log(\mathcal{K} \mathcal{Q}))$	(OMP.3)
Least-squares projection	$\mathcal{O}(\mathcal{J} ^3)$	(OMP.4)
Stopping criterion	$\mathcal{O}(nP \mathcal{J})$	(OMP.5)
MF receiver	Complexity	Remarks
Correlations $z_{i,k,q}[n]$	$\mathcal{O}(nMI \mathcal{K} \mathcal{Q})$	Eq. (8)
Path selection	$\mathcal{O}(nIR \log(\mathcal{K} \mathcal{Q}))$	
Accumulation	$\mathcal{O}(nI \mathcal{K} \mathcal{Q})$	MMV mode

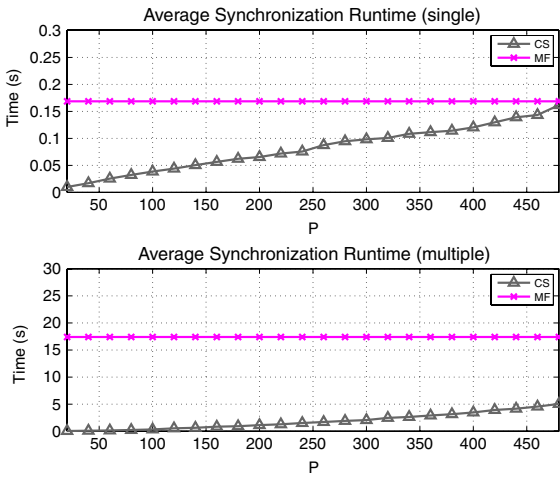


Fig. 7. Average runtime to evaluate $\{\hat{f}, \hat{q}, \hat{k}\}$ from a received observation vector $\mathbf{y}[n]$ for the compressive scheme, with $n = 1$ (above) and $n = 50$ (below) as a function of $P = \{20, 40, \dots, 480\}$, and compared against the MF receiver. Each curve was run separately on a 64-bit i7 920 CPU running at 2.67 GHz.

mainly determined by the number of additions to compute the correlations, leading to $\mathcal{O}(nMI|\mathcal{K}||\mathcal{Q}|)$. For hardware implementation this is attractive since the filterbank processing does not require complex multiplications. However, a similar saving can be added to the CS receiver by appropriately designing \mathbf{B} such that $\{\psi_p[m]\}$ also has ± 1 elements.

The comparison between the dominant terms results in a CS to MF complexity ratio $(P/I|\mathcal{K}||\mathcal{Q}| + P|\mathcal{J}|/M)$ that favors the former and emphasizes the complexity savings. In fact, one should expect $P|\mathcal{J}| \ll M$ and $P \ll I|\mathcal{K}||\mathcal{Q}|$, which shows that the CS gains by removing its dependency on the length of the C/A sequence. This trend is also highlighted in Fig. 7 by the average CPU time spent while executing the steps described in Table 1.

When $n > 1$ the ratio remains unchanged since all the additional steps (Table 1) for the ReMBo technique require marginal increase of operations. When compared to $n = 1$, the MF spends more CPU time to accumulate the correlation outputs whereas the CS receiver experiences a

reverse trend. The additional effort³ spent to evaluate \mathbf{R}_{cc} is compensated by less operations within the OMP algorithm, and results in a gain in efficiency as highlighted in Table 1.

In general, knowing a priori the order $|\mathcal{J}|$ the CS receiver has an advantage over the MF, which is true and practical in GPS systems because the order of number of active satellites in the field of view is actually known. However, the MF approach always explores and ranks all the $|\mathcal{K}||\mathcal{Q}|$ dimensions for every satellite before selecting $|\mathcal{J}|R$.

8. Conclusions

We proposed a compressive multichannel acquisition scheme for GPS receivers that lowers greatly the complexity. The reduction is achieved by choosing linear combinations of all the MFs, which leads to great savings in practice. As shown in the analysis and numerical results, our scheme can efficiently recover the unknown delay-Doppler pairs using significantly fewer correlators than those needed in a standard GPS receiver. Regardless of the sparse recovery algorithm, the acquisition performance improves gracefully with the increase of acquisition channels and the number of observations. Therefore, although the proposed scheme has a performance loss in terms of RMSE and success rate compared to the standard GPS scheme, it provides a design tool to trade-off complexity and performance that can be useful to scale down the cost and energy consumption of GPS chips.

Appendix. Proof of Theorem 1

In this proof, we prove the structure of the matrices $\mathbf{M}_{\phi\phi}(\omega, \mathbf{k}, \mathbf{q})$ and $\mathbf{M}_{\phi\phi}(\omega, \mathcal{K}, \mathcal{Q})$, which will lead to the results of the proposed theorem. Let $\phi_{i,k,q}(-t) = \phi_i(t - qT_c)e^{ik\Delta\omega t}$. Denote by $\Phi_{i,k,q}(\omega) = \Phi_i(\omega - k\Delta\omega)e^{-i(\omega - k\Delta\omega)qT_c}$ the Fourier transform of $\phi_{i,k,q}(-t)$.

Using $\Phi_i(\omega) = G(\omega) \sum_{m=0}^{M-1} s_i[m]e^{-im\omega T_c}$ together with $G(\omega) = [1 + \epsilon_g(\omega)]\text{rect}_{2\pi L/T_c}(\omega)$ and ignoring higher

³ Note that in practice, the covariance and SVD computation can be optional by directly choosing a set of measurements $\{\mathbf{c}[n]\}$ and solve the MMV system formed using that set of measurements instead.

order perturbations $\mathcal{O}(|\epsilon_g(\omega)|^2)$, we can write the $[(i', k, q), (i, r)]$ th entry of the matrix $\mathbf{M}_{\phi\phi}(\omega, \mathbf{k}, \mathbf{q})$ over $\omega \in [-\pi/T, \pi/T]$ according to (12) as

$$\begin{aligned} & [\mathbf{M}_{\phi\phi}(\omega, \mathbf{k}, \mathbf{q})]_{(i', k, q), (i, r)} \\ &= \frac{1}{T} e^{i\omega(q-q_{i,r})T_c} e^{-i(kq-k_{i,r}q_{i,r})\Delta\omega T_c} \sum_{\ell=0}^{LM-1} e^{-i\frac{2\pi\ell}{T}(q-q_{i,r})T_c} \\ & \quad \times \sum_{m'=0}^{M-1} \sum_{m=0}^{M-1} s_{i'}^*[m'] s_i[m] e^{i\omega(m'-m)T_c} e^{-i\frac{2\pi\ell}{T}(m'-m)T_c} \\ & \quad \times e^{-i\Delta\omega T_c(m'k-mk_{i,r})} + \mathcal{O}(\epsilon_g(\omega)). \end{aligned} \quad (\text{A.1})$$

With a change of variable $u = m - m'$, we can re-write the double summations over m and m' as

$$\begin{aligned} & \sum_{m'=0}^{M-1} \sum_{m=0}^{M-1} s_{i'}^*[m'] s_i[m] e^{i\omega(m'-m)T_c} e^{-i\frac{2\pi\ell}{T}(m'-m)T_c} \\ & \quad \times e^{-i\Delta\omega T_c(m'k-mk_{i,r})} \\ &= \sum_{u=-M+1}^{M-1} M \cdot \frac{1}{M} \sum_{m=0}^{M-1} s_{i'}^*[m-u] s_i[m] e^{-i\Delta\omega T_c(k-k_{i,r})m} \\ & \quad \times e^{-iu(\omega-k\Delta\omega-\frac{2\pi\ell}{T})T_c}, \end{aligned} \quad (\text{A.2})$$

where $R_{i'}[u, k - k_{i,r}]$ is the ambiguity function between the sequences $\{s_{i'}[m]\}$ and $\{s_i[m]\}$ perturbed by phase-shifts determined by the mismatch of the Doppler shift $e^{-i\Delta\omega T_c(k-k_{i,r})m}$.

To evaluate the ambiguity function, we first note that in the absence of Doppler mismatch, namely $k = k_{i,r}$ we have

$$\begin{aligned} & R_{i'}[u, k - k_{i,r}] \\ &= \frac{1}{M} \sum_{m=0}^{M-1} s_{i'}^*[m-u] s_i[m] = R_{i'}[u], \quad k = k_{i,r} \end{aligned} \quad (\text{A.3})$$

where $R_{i'}[u]$ is the C/A code cross-correlation in (4). The MLS code [7] and Gold code [16] has been demonstrated to have low correlation $R_{i'}[u] = \mathcal{O}(1/M)$ over time shifts $u \neq 0$ and/or $i \neq i'$ as indicated by the cross spectral density (5). It is further desirable for $R_{i'}[u, k - k_{i,r}]$ to decay rapidly over k such that dominant values only appear when $k = k_{i,r}$. By choosing $\Delta\omega = 2\pi j/T, j \in \mathbb{Z}^+$, we have at $u = 0$ and $i = i'$ that

$$\begin{aligned} & \frac{1}{M} \sum_{m=0}^{M-1} e^{-i\Delta\omega T_c(k-k_{i,r})m} = \frac{1}{M} \sum_{m=0}^{M-1} e^{-i\frac{2\pi jm}{M}(k-k_{i,r})} \\ &= \delta[k - k_{i,r}]. \end{aligned} \quad (\text{A.4})$$

Next, we examine the ambiguity function for any pair of codes i and i' in the presence of Doppler mismatch $k \neq k_{i,r}$. As shown in Fig. A.8, the ambiguity function remains well concentrated at $i = i', u = 0$ and $k = k_{i,r}$. Since the ambiguity functions of all the codes used by different satellites exhibit similar decay behaviors, we here show the ambiguity functions of four arbitrary pairs of Gold codes with $i = 13$ against $i' = 13, 16, 19, 22$ over $u = -M + 1, \dots, M - 1$ with $M = 1023$ and $k - k_{i,r} = -K, \dots, K$ with $K = 20$ (i.e., ± 10 kHz

Doppler shifts). By evaluating numerically the values of the ambiguity functions over different time shifts u and Doppler shifts k , it is found that except for $i = i', u = 0$ and $k = k_{i,r}$, few large magnitudes $R_{i'}[u, k - k_{i,r}] \approx 70/M$ appear while typical values range from $1/M$ to $5/M$. Therefore together with (A.3) and (A.4), we express the ambiguity function as follows

$$R_{i'}[u, k - k_{i,r}] = \begin{cases} 1, & u = 0, k = k_{i,r}, i = i' \\ \mathcal{O}\left(\frac{1}{M}\right), & \text{otherwise,} \end{cases} \quad (\text{A.5})$$

where $\mathcal{O}(1/M)$ is some small perturbation. This fact is well known [21], which is why here we only provide the intuition and not a rigorous proof.

Since the matrix entry contains significant values only if $k = k_{i,r}$ (i.e., $R_{i'}[u, k - k_{i,r}] = R_{i'}[u]$),

$$\begin{aligned} & [\mathbf{M}_{\phi\phi}(\omega, \mathbf{k}, \mathbf{q})]_{(i, k_{i,r}, q), (i, r)} \\ &= \frac{M}{T} e^{i\omega(q-q_{i,r})T_c} e^{-ik_{i,r}(q-q_{i,r})\Delta\omega T_c} \sum_{\ell=0}^{LM-1} e^{-i\frac{2\pi\ell}{T}(q-q_{i,r})T_c} \\ & \quad \times \underbrace{\sum_{u=-M+1}^{M-1} R_{i'}[u] e^{-iu(\omega-k\Delta\omega-\frac{2\pi\ell}{T})T_c}}_{\triangleq S_{i'}(e^{i(\omega-k\Delta\omega-\frac{2\pi\ell}{T})T_c})} + \mathcal{O}(\epsilon_g(\omega)) + \mathcal{O}(1). \end{aligned}$$

Using the spectrum $S_{i'}(e^{i\omega T_c}) = \delta[i' - i] + \epsilon_{i',i}(\omega)$ and ignoring higher order perturbations $\mathcal{O}(|\epsilon_{i',i}(\omega)|^2)$, the non-zero entries of the matrix $\mathbf{M}_{\phi\phi}(\omega, \mathbf{k}, \mathbf{q})$ are explicitly written as

$$\begin{aligned} & [\mathbf{M}_{\phi\phi}(\omega, \mathbf{k}, \mathbf{q})]_{(i', k_{i,r}, q), (i, r)} \\ &= \frac{M}{T} e^{i\omega(q-q_{i,r})T_c} e^{-ik_{i,r}(q-q_{i,r})\Delta\omega T_c} \sum_{\ell=0}^{LM-1} e^{-i\frac{2\pi\ell}{T}(q-q_{i,r})T_c} \\ & \quad + \mathcal{O}(\epsilon_g(\omega)) + \mathcal{O}(\epsilon_{i',i}(\omega)) + \mathcal{O}(1). \end{aligned}$$

With $T = MT_c$, we use the property

$$\frac{1}{T} \sum_{\ell=0}^{LM-1} e^{-i\frac{2\pi\ell}{T}(q-q_{i,r})T_c} = L\delta[q - q_{i,r}] \quad (\text{A.6})$$

to further express the non-zero entries of $\mathbf{M}_{\phi\phi}(\omega, \mathbf{k}, \mathbf{q})$ at $i' = i, k = k_{i,r}$ and $q = q_{i,r}$

$$\begin{aligned} & [\mathbf{M}_{\phi\phi}(\omega, \mathbf{k}, \mathbf{q})]_{(i, k_{i,r}, q_{i,r}), (i, r)} \\ &= LM + \mathcal{O}(\epsilon_g(\omega)) + \mathcal{O}(\epsilon_{ii}(\omega)) + \mathcal{O}(1), \\ & \quad \omega \in [-\pi/T, \pi/T]. \end{aligned} \quad (\text{A.7})$$

Similarly, the matrix $\mathbf{M}_{\phi\phi}(\omega, \mathcal{K}, \mathcal{Q})$ has significant entries only when $i = i', k = k'$ and $q = q'$

$$\begin{aligned} & [\mathbf{M}_{\phi\phi}(\omega, \mathcal{K}, \mathcal{Q})]_{(i', k, q), (i, k, q)} \\ &= LM + \mathcal{O}(\epsilon_g(\omega)) + \mathcal{O}(\epsilon_{i',i}(\omega)) + \mathcal{O}(1). \end{aligned} \quad (\text{A.8})$$

Since the error functions satisfy $\|\epsilon_g(\omega)\| \ll 1$ and $\|\epsilon_{i',i}(\omega)\| \ll 1$, the results in Theorem 1 follow.

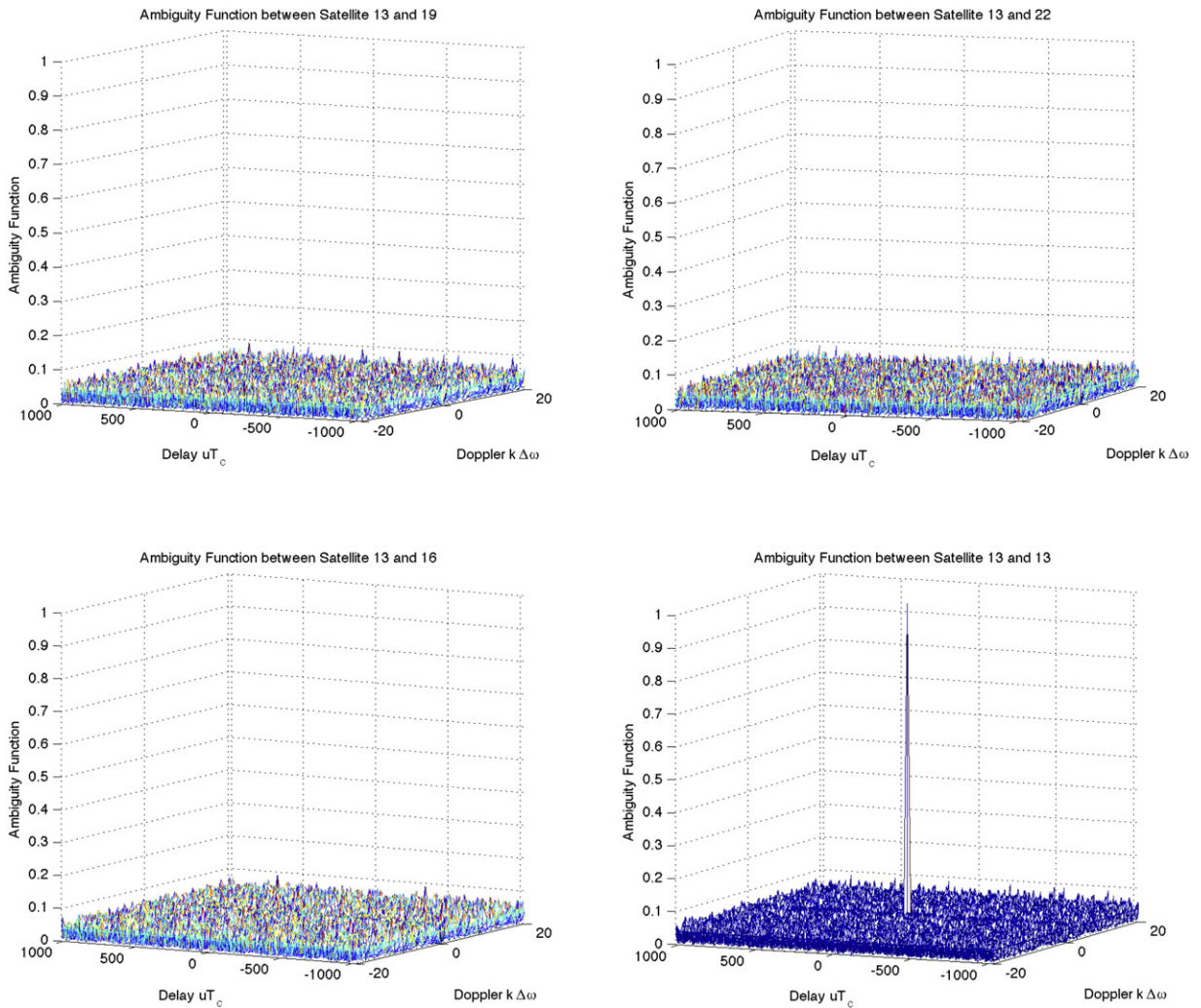


Fig. A.8. $R_{\ell i}[u, k]$ with $i = 13$ against $i' = 13, 16, 19, 22$.

References

- [1] E.D. Kaplan, Understanding GPS: Principles and Applications, second edition, Artech House Publisher, 2006.
- [2] M.S. Braasch, A.J.V. Dierendonck, GPS receiver architectures and measurements, Proc. IEEE 87 (1) (1999) 48–64.
- [3] J-C. Auber, A. Bibaut, J-M. Rigal, Characterization of Multipath on Land and Sea at GPS Frequencies, Thomson CSF-Detexis, France, 1995.
- [4] S. Ohmori, H. Wakana, S. Kawase, Mobile Satellite Communications, Artech House, Norwell, MA, 1996.
- [5] P.W. Ward, GPS receiver interference monitoring, mitigation and analysis techniques, J. Inst. Navigation 41 (4) (1995) 367–391. Winter.
- [6] M. Sahnoudi, M. Amin, Robust synchronization of weak GPS signals in multipath and jamming environments, Signal Process. 89 (7) (2009).
- [7] J. Soubielle, I. Fijalkow, P. Duvaut, A. Bibaut, GPS positioning in a multipath environment, IEEE Trans. Signal Process. 50 (10) (2002).
- [8] P.K. Enge, The global positioning system: signals, measurements, and performance, Int. J. Wireless Inform. Networks 1 (2) (1994).
- [9] B.R. Townsend, P. Fenton, A practical approach to the reduction of pseudorange multipath errors in a L1 GPS receiver, in: Proc. ION GPS-94, Salt Lake City, USA, 1994.
- [10] R.D.J. Van Nee, et al. The multipath estimating delay lock loop: approaching theoretical accuracy limits, in: Proc. IEEE PLANS, Apr. 1994.
- [11] E. Candès, J. Romberg, T. Tao, Stable signal recovery from incomplete and inaccurate measurements, Commun. Pure Appl. Math. 59 (8) (2006) 1207–1223.
- [12] Y.C. Eldar, Compressed sensing of analog signals in shift-invariant spaces, IEEE Trans. Signal Process. 57 (8) (2009) 2986–2997.
- [13] M. Mishali, Y.C. Eldar, Reduce and boost: recovering arbitrary sets of jointly sparse vectors, IEEE Trans. Signal Process. 56 (10) (2008) 4692–4702.
- [14] S.F. Cotter, B.D. Rao, K. Engan, K. Kreutz-Delgado, Sparse solutions to linear inverse problems with multiple measurement vectors, IEEE Trans. Signal Process. 53 (7) (2005) 2477–2488.
- [15] J. Chen, X. Huo, Theoretical results on sparse representations of multiple-measurement vectors, IEEE Trans. Signal Process. 54 (12) (2006) 4634–4643.
- [16] R. Gold, Optimal binary sequences for spread spectrum multiplexing, IEEE Trans. Information Theory 13 (4) (1967) 619–621.
- [17] K. Gedalyahu, Y.C. Eldar, Time-delay estimation from low-rate samples: a union of subspaces approach, IEEE Trans. Signal Process. 58 (6) (2010) 3017–3031.
- [18] R. Calderbank, S. Howard, S. Jafarpour, Construction of a large class of deterministic sensing matrices that satisfy a statistical isometry property, IEEE J. Select. Topics Signal Process. 4 (2) (2010) 358–374.
- [19] Y.C. Pati, R. Rezaifar, P.S. Krishnaprasad, Orthogonal matching pursuit: recursive function approximation with applications to wavelet decomposition, Asilomar Conf. Signals, Systems Computers 1 (1993) 40–44.

- [20] P. Conon, G.H. Golub, Tracking a few extreme singular values and vectors in signal processing, *IEEE Process.* 78 (1990) 1327–1343.
- [21] T.B. Hale, M.A. Temple, B.L. Crossley, Ambiguity analysis for pulse compression radar using gold code sequences, in: *Proceedings of the 2001 IEEE Radar Conference*, 2001, 2001, pp. 111–116.



Xiao Li received the B.Eng. Degree (2007) with highest honor in Electrical Engineering from Sun Yat-Sen (Zhongshan) University (Guangzhou, China), where he was awarded 4-year scholarships for comprehensive excellence. From 2007 to 2009, he obtained full scholarship (postgraduate studentship) to study the M.Phil. Degree in Electrical and Electronic Engineering from The University of Hong Kong. After obtaining the M.Phil. Degree, he started pursuing the Ph.D. Degree at University of California, Davis from 2009

Fall. His research interests include statistical signal processing, optimization, sub-Nyquist sampling and compressed sensing, in-network processing and applications in communications, wireless technology and power grid.



Andrea Rueetschi received a Diploma in Physical Electronics from the University of Neuchâtel (IMT—Institute of a Microengineering, Neuchâtel, Switzerland) in March 1997. From November 1997 until December 2007 he worked as an ASIC design engineer for Philips Semiconductors (Zürich, Switzerland and San Jose, CA), RF Micro Devices (formerly Resonext Communications, San Jose, CA) and Marvell Semiconductors (Santa Clara, CA) developing DSP modules for wireless applications like IEEE 802.11 or IS-95.

From January 2008 he joined the graduate program (PhD) at Cornell University (Ithaca, NY) and transferred to UC Davis in January 2009.



Yonina C. Eldar (IEEE S'98-M'02-SM'07) received the B.Sc. Degree in physics and the B.Sc. Degree in electrical engineering both from Tel-Aviv University (TAU), Tel-Aviv, Israel, in 1995 and 1996, respectively, and the Ph.D. Degree in electrical engineering and computer science from the Massachusetts Institute of Technology (MIT), Cambridge, in 2002.

From January 2002 to July 2002, she was a Postdoctoral Fellow at the Digital Signal Processing Group at MIT. She is currently a Professor in the Department of Electrical Engineering at the Technion-Israel Institute of Technology, Haifa. She is also a Research Affiliate with the Research Laboratory of Electronics at MIT and a Visiting Professor at Stanford University, Stanford, CA. Her research interests are in the broad

areas of statistical signal processing, sampling theory and compressed sensing, optimization methods, and their applications to biology and optics.

Dr. Eldar was in the program for outstanding students at TAU from 1992 to 1996. In 1998, she held the Rosenblith Fellowship for study in electrical engineering at MIT, and in 2000, she held an IBM Research Fellowship. From 2002 to 2005, she was a Horev Fellow of the Leaders in Science and Technology program at the Technion and an Alon Fellow. In 2004, she was awarded the Wolf Foundation Krill Prize for Excellence in Scientific Research, in 2005 the Andre and Bella Meyer Lectureship, in 2007 the Henry Taub Prize for Excellence in Research, in 2008 the Hershel Rich Innovation Award, the Award for Women with Distinguished Contributions, the Muriel & David Jacknow Award for Excellence in Teaching, and the Technion Outstanding Lecture Award, in 2009 the Technions Award for Excellence in Teaching, and in 2010 the Michael Bruno Memorial Award from the Rothschild Foundation. She is a member of the IEEE Signal Processing Theory and Methods technical committee and the Bio Imaging Signal Processing technical committee, an Associate Editor for the IEEE TRANSACTIONS ON SIGNAL PROCESSING, the EURASIP Journal of Signal Processing, the SIAM Journal on Matrix Analysis and Applications, and the SIAM Journal on Imaging Sciences, and on the Editorial Board of Foundations and Trends in Signal Processing.



Anna Scaglione (IEEE F10⁺) received the Laurea (M.Sc. Degree) in 1995 and the Ph.D. Degree in 1999 from the University of Rome, “La Sapienza”. She is currently Professor in Electrical and Computer Engineering at University of California at Davis, where she joined in 2008. She was previously at Cornell University, Ithaca, NY, from 2001 where became Associate Professor in 2006; prior to joining Cornell she was Assistant Professor in the year 2000–2001, at the University of New Mexico. She served as

Associate Editor for the IEEE Transactions on Wireless Communications from 2002 to 2005, and serves since 2008 the Editorial Board of the IEEE Transactions on Signal Processing from 2008, where she is Area Editor. She has co-organized several special sessions in signal processing and communication conferences; she has served in the past as guest editor for the Communication Magazine and the Journal on Selected Topics in Signal Processing and she is currently serving as guest editor for the Journal on Selected Areas in Communications, for a series of special issues on Smartgrid. She was in the Signal Processing for Communication Committee from 2004 to 2009. She was general chair of the workshop SPAWC 2005 and keynote speaker in SPAWC 2008 and ISPLC 2010. Dr. Scaglione received the 2000 IEEE Signal Processing Transactions Best Paper Award the NSF Career Award in 2002 and she is co-recipient of the Ellersick Best Paper Award (MILCOM 2005). Her expertise is in the broad area of signal processing for communication systems and networks. Her current research focuses on communication and wireless networks, sensors' systems for monitoring, control and energy management and network science.